arXiv:1805.03823v1 [physics.atom-ph] 10 May 2018

Spatial dynamics analysis of polarized atom vapor

X.Y.Hu,[1] H.F.Dong,[1] H.C.Huang,[1] L.Chen,[1] and Y.Gao[1]
School of Instrumentation Science and Opto-Electronics Engineering, Beihang University, Beijing 100191, China.

(Dated: 16 March 2022)

We analyze the spatial dynamics of polarized atom vapor and present a mathematical method to eliminate the diffusion effect partially. It is found that the diffusion effect of polarized atoms can be regarded as a low pass filter in spatial frequency domain and fits well with a Butterworth filter. The fitted spatial filter can be used to restore the original magnetic image before being blurred by the diffusion, thus improving the magnetic spatial resolution. The results of spatial dynamics simulation and magnetic image restoration show the potential usage of this method in magnetic gradiometer and atomic magnetic microscopy.

PACS numbers: 78.20.Ls, 87.57.nf
Keywords: Bloch equation; spatial dynamics; magnetometer; diffusion; polarized atom

I. INTRODUCTION

The temporal and spatial dynamics of polarized atom vapor is described by Bloch equation[1], which is the basic model in fields such as nuclear magnetic resonance(NMR)[2,3], atomic magnetometer[4–6] and atomic gyroscopes[7,8]. In these applications the temporal dynamics of polarized atom vapor is analyzed theoretically and verified experimentally. As most of the applications measure the average polarization of atoms in the vapor cell, the spatial dynamics is usually ignored in the modeling and analysis. In the case of gradiometer or array measurements, the diffusion is thought as the essential limit for the spatial resolution[9–11].

Inspired by the work of D. Giel et al, who pointed out that the space-time evolution of polarization can be expanded in terms of spatial periodic functions[10], we introduce the spatial frequency response of the input magnetic field, which can describe the spatial dynamics of polarized atom vapor in nonuniform magnetic field. MATLAB Simulink is used to simulate the polarized atom vapor system. By setting the magnetic field distribution as one dimensional (1D) sinusoidal waves with different spatial frequency, we get the evolution of the atom polarization in both time and space domain. The result shows that the response decreases when spatial frequency of magnetic field increases, just like a low pass spatial filter, which can be fitted well to a Butterworth filter. Assuming the diffusion effect is isotropy, it can be expanded directly to a two dimensional (2D) spatial filter. By reversing the 2D filter, we obtain a 2D high pass filter that can be used to eliminate diffusion effect and restore the original image partially.

The paper is organized as follows: After a brief introduction of background and motivation in section I, Section II describes the model and parameters calculation used in the simulation. Section III illustrates and discusses the results of spatial dynamics simulation. Finally, conclusions are summarized in section IV.

II. MODELING AND PARAMETERS

The Bloch equation can be written with diffusion term as following[12,13]:

$$\frac{\partial}{\partial t}\overrightarrow{P} = D\nabla^2\overrightarrow{P} + \gamma\overrightarrow{B}\times\overrightarrow{P} + R_p(s-\overrightarrow{P}) - \frac{\overrightarrow{P}}{T_1,T_2} \quad (1)$$

where $\overrightarrow{P}$ is the polarization of alkali atoms, D is the diffusion coefficient, γ is the gyromagnetic ratio, $\overrightarrow{B}$ is the magnetic field, R_p is the pumping rate and T_1 and T_2 are the relaxation times for polarization components parallel and transverse to $\overrightarrow{B}$, respectively. The four terms on the right-hand side describe diffusion, precession, pumping and relaxation, respectively.

To simplify Eq1 and obtain the numerical result of spatial dynamics, we assume the pumping beam and the probing beam are along z axis and x axis, respectively, and the direction of the magnetic field is along y axis. Besides, we also suppose that atoms are fully polarized using a high power short pulse beam. The polarization vector precesses freely in x−z plane after the pumping pulse. In this condition, P_y, T_1 and R_p can be ignored and Eq.(1) can be simplified as below:

$$\frac{\partial}{\partial t}\begin{bmatrix}P_x\\P_z\end{bmatrix} = D\nabla^2\begin{bmatrix}P_x\\P_z\end{bmatrix} + \gamma B_y\begin{bmatrix}-P_z\\P_x\end{bmatrix} - R_r\begin{bmatrix}P_x\\P_z\end{bmatrix} \quad (2)$$

where relaxation rate $R_r = 1/T_2$ and diffusion coefficient D can be calculated according to the experimental setup.

Considering that the atom vapor cell can be antirelaxation coated, or buffered with high pressure gas and can work under spin-exchange relaxation free (SERF) regime, wall collision relaxation and spin-exchange relaxation can be neglected. Moreover, as we measure the local field instead of the average field in the vapor cell, gradient broadening can also be ignored. So the relaxation rate R_r is mainly decided by the spin destruction[14],

$$R_r \approx R_s d = \bar{v}_\alpha\sigma_\alpha^{sd}n_\alpha + \bar{v}_q\sigma_q^{sd}n_q + \bar{v}_b\sigma_b^{sd}n_b \quad (3)$$

where the first term denotes the collision between alkali atoms themselves, the second term denotes the quench

collision and the third term denotes the collision between alkali atom and buffer gas atom. $\bar{v}, \sigma^{sd}$ and n are the relative velocity, collision cross-section of collision pair and density of atoms, respectively. The subscripts α, q and b are for alkali atoms, quenching gas atoms and buffer gas atoms, respectively. The diffusion coefficient depends on the temperature and the pressure of the gas[10],

$$D = D_0 \left(\frac{P_0}{P}\right)\left(\frac{T}{T_0}\right)^{3/2} \tag{4}$$

where $T_0 = 273.15K$ is the standard temperature, $P_0 = 760Torr$ is the standard pressure and D_0 is the standard diffusion coefficient at T_0 and P_0. Standard diffusion coefficients of Cesium atom in He and N_2 are $0.39cm^2/s$[15] and $0.087(15)cm^2/s$[16], respectively, which are used in our choice of D in section III.

III. NUMERICAL SIMULATION AND RESULTS ANALYSIS

A. Spatial frequency response simulation

In the simulation, $R_r = 300s^{-1}$ and D = $0 \sim 1cm^2/s$ are choosed according to section II with typical parameters in the atom vapor polarization experiments. And to obtain the spatial frequency response we set B_y as a magnetic field with spatial sinusoidal distribution on z axis and $B_x = B_z = 0$. Thus the input magnetic field can be written as

$$B_y(z) = B_0 \sin(\omega z) \tag{5}$$

where B_0 is the magnetic amplitude, ω is the spatial angular frequency and z is the spatial position along z axis.

By simulating the model in Eq.(2) with diffusion term, we can get the temporal and spatial polarization $\hat{P}_x(z, t_d)$. Then the output magnetic field can be calculated by,

$$\hat{B}_y(z) = \frac{\arcsin(-\hat{P}_x(z, t_d)e^{R_r t_d})}{2\pi\gamma t_d} \tag{6}$$

pulse pumping magnetometer for different D and ω. Time delay $t_d = 10\mu s$ and relaxation rate $R_r = 300s^{-1}$.

According to our simulation, $\hat{B}_y(z, t_d)$ also follows the sinusoidal distribution with the same spatial frequency, i.e., $\hat{B}_y(z) \approx \hat{B}_0 \sin(\omega z)$.We get the corresponding magnetic amplitude $\hat{B}_0$ of different ω, t_d and D. With a certain time delay t_d the amplitude magnification $\hat{B}_0/B_0$ decreases when spatial angular frequency ω increases, as shown in Fig.1. The figure also shows that the cutoff spatial frequency of the system decreases with the increase of diffusion coefficient.

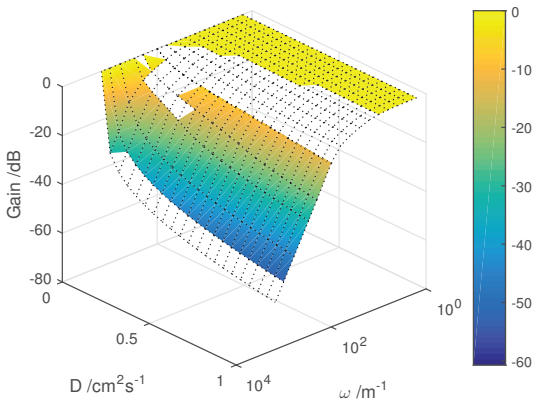
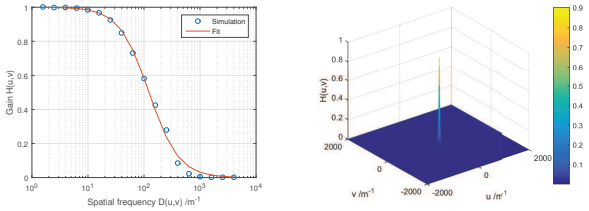


FIG. 1. (Color Online) Amplitude response of the short pulse pumping magnetometer for different D and ω. Time delay t_d=10s and relaxation rate $R_r = 300s^{-1}$.



(a) (b)

FIG. 2. (Color Online) (a) The spatial frequency response when t_d=10s and D = $0.6cm^2/s$. (b) The plot of the 2D filter generated by the fit curve in (a).

B. Reverse approximation of diffusion process

Fig.2(a) is the spatial response when $t_d = 10\mu$s and $D = 0.6\text{cm}^2/\text{s}$, which can be fitted well with a Butterworth filter $1/\sqrt{1 + (\omega/\omega_0)^{2n}}$. The phase response of Butterworth filter is ignored due to the isotropy of diffusion. The corresponding 2D Butterworth filter can be expressed as

$$H(u, v) = \frac{1}{1 + (D(u, v)/D_0)^{2n}} \tag{7}$$

where $D(u, v)$ is the distance between a point (u, v) in the frequency domain and the center of the frequency rectangle, and D_0 is the cutoff frequency[17]. Fig. 2(b) illustrates the corresponding 2D spatial filter, which is expanded from the fitted curve of Fig. 2(a).

As the 2D filter in Fig. 2(b) is generated by the spatial frequency response of Bloch equation simulation, it approximately represents the diffusion effect. Furthermore, we can restore the original magnetic image with a reversed 2D filter $1 - H(u, v)$ in Fig. 2(b).

To provide a better view of the restoration effect, we simulate the atom vapor system in magnetic field of two close magnetic dipoles, and assume the dipoles is small

enough to ignore the magnetic field inside the dipoles. The magnetic field B_y vaires inversely with the third power of distance in $y-z$ plane, as show in Fig.3(a) . The measured magnetic image simulated using Bloch

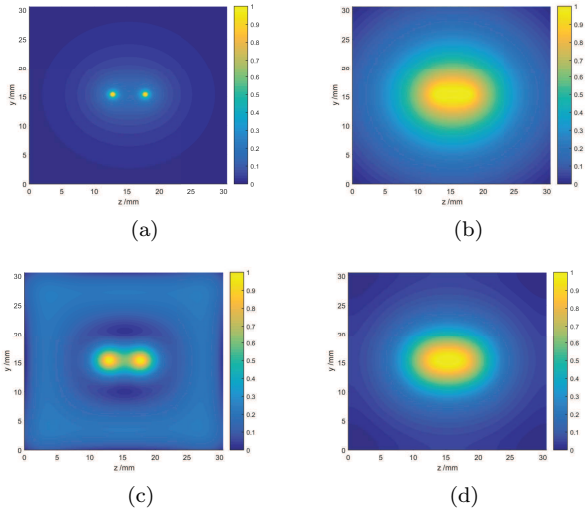


FIG. 3. (Color Online) (a) The original magnetic field of two dipoles in $y-z$ plane. The distance between the two dipoles is 5mm. (b) The measured magnetic field, where the dipoles can hardly be distinguished due to diffusion. This image is calculated using the simulation result of P_x and Eq.(6). (c) The restored magnetic field using reversed 2D filter $1-H(u,v)$. (d) Filtered image from (a), with filter $H(u,v)$ applied. To provide a better view, all of these images are normalized.

model, i.e. Eq.(2), and 2D filter, i.e. Eq.(7), are displayed in Fig. 3(b) and Fig. 3(d), respectively, where the two dipoles can hardly be distinguished. With a reversed 2D filter $1-H(u,v)$, we get the restored image from Fig. 4 and the result is shown in Fig. 3(c). In the restored image, the two dipoles can be distinguished again and thus the spatial resolution is improved. The slightly diffrence between Fig. 3(a) and Fig. 3(c) may be due to the fit error in the high frequency part.

IV. CONCLUSION

In summary, the spatial dynamics of polarized atom vapor is analyzed based on the Bloch equation and short pulse pumping and probe scheme. The simulated spatial frequency response fits well with a low pass Butterworth filter. By passing the magnetic image through the reversed spatial fitter, we eliminate partially the diffusion effect and increase the spatial resolution of the image. This analysis and restoration method can be used in spatial magnetometry, such as magnetic gradiometer and atomic magnetic microscopy.

ACKNOWLEDGEMENT

The authors thank the support by National Natural Science Foundation of China under Grant No. 61074171 and 61273067 and National Program on Key Basic Research Project of China (2012CB934104). The authors would like to thank Dr. Iannis K. Kominis for the beneficial discussion on spatial resolution, which is another great inspiration to the idea of this paper.

REFERENCES

[1] F. Bloch, W. W. Hansen, and M. Packard, "Nuclear induction," *APS Journals*, **69** (1946).
[2] W. S. Hinshaw and A. H. Lent, "An introduction to nmr imaging: From the bloch equation to the imaging equation," Proceedings of the IEEE **71**, 338–350 (1983).
[3] R. H. Lehmberg, "Modification of bloch's equations at optical frequencies," Optics Communications **5**, 152–156 (1972).
[4] I. Savukov, "Gradient-echo 3d imaging of rb polarization in fiber-coupled atomic magnetometer," Journal of Magnetic Resonance **256**, 9–13 (2015).
[5] J. C. Allred, R. N. Lyman, T. W. Kornack, and M. V. Romalis, "High-sensitivity atomic magnetometer unaffected by spin-exchange relaxation." Physical Review Letters **89**, 130801 (2002).
[6] J. Fang, T. Wang, H. Zhang, Y. Li, and S. Zou, "Optimizations of spin-exchange relaxation-free magnetometer based on potassium and rubidium hybrid optical pumping," Review of Scientific Instruments **85**, 123104 (2014).
[7] H. Dong, J. Fang, J. Qin, and Y. Chen, "Analysis of the electrons-nuclei coupled atomic gyroscope," Optics Communications **284**, 2886–2889 (2011).
[8] T. W. Kornack, R. K. Ghosh, and M. V. Romalis, "Nuclear spin gyroscope based on an atomic comagnetometer," Physical Review Letters **95**, 230801 (2005).
[9] I. K. Kominis, T. W. Kornack, J. C. Allred, and M. V. Romalis, "A subfemtotesla multichannel atomic magnetometer," Nature **422**, 596–599 (2003).
[10] D. Giel, G. Hinz, D. Nettels, and A. Weis, "Diffusion of cs atoms in ne buffer gas measured by optical magnetic resonance tomography," Optics Express **6**, 251–6 (2000).
[11] K. Kim, S. Begus, H. Xia, S. K. Lee, V. Jazbinsek, Z. Trontelj, and M. V. Romalis, "Multi-channel atomic magnetometer for magnetoencephalography: A configuration study," Neuroimage **89**, 143–151 (2014).
[12] M. P. Ledbetter, I. M. Savukov, V. M. Acosta, D. Budker, and M. V. Romalis, "Spin-exchange-relaxation-free magnetometry with cs vapor," Phys. Rev. A **77**, 033408 (2008).
[13] H. C. Torrey, "Bloch equations with diffusion terms," Phys. Rev. **104**, 563–565 (1956).
[14] T. W. Kornack, "A test of cpt and lorentz symmetry using a potassium-helium-3 co-magnetometer," (2006).
[15] K. Ishikawa, Y. Anraku, Y. Takahashi, and T. Yabuzaki, "Optical magnetic-resonance imaging of laser-polarized cs atoms," J. Opt. Soc. Am. B **16**, 31–37 (1999).
[16] M. S. Manalis, "Nonthermal saha equation and the physics of a cool dense helium plasma," Phys. Rev. A **5**, 993–994 (1972).
[17] R. C. Gonzalez and R. E. Woods, *Digital Image Processing* (Pearson Education Asia ltd, 2009).